Supporting Information for

Enhancing the hydrogen evolution activity of diiron molecular electrocatalyst by modulating substituent effect of carbon nanotubes

Pei-Hua Zhao*, Shao-Jie Wang, Fan-Zeng Wei, Xue Su and Hui Gao

School of Materials Science and Engineering, North University of China, Taiyuan 030051, P. R. China

*Corresponding author.

Email: zph2004@nuc.edu.cn (P.-H. Zhao).

Contents:

P18. **Figure S8.** Chronoamperometry (CA) experiment of the **CNT-N-ADT** (red) , **CNT-C-ADT** (green) , and **CNT-O-ADT** (red) electrodes with the same loading of 0.74 mg cm^{-2} consumed charge – time during 5 h electrolysis in 0.1 M phosphate buffer (pH = 7) aqueous solutions at the respective applied potentials of -0.88 V vs RHE.

P19. **Table S3.** Relevant CA data of **CNT-X-ADT** (X = N, C, O) in pH = 7 aqueous solution

I. Materials and methods

All reactions were performed under a dry and oxygen-free atmosphere with a standard Schlenk operation. Dicyclohexylcarbodiimide (DCC), 4-dimethylaminopyridine (DMAP), *p*-hydroxybenzaldehyde (HOC_6H_4CHO-*p*), N-methylglycine (sarcosine, $MeNH(CH_2CO_2H)$), pristine multi-walled carbon nanotube (MWCNT-COOH, 2.56 wt%-COOH, purity > 85%, main particle size range < 3nm), 0.1 M potassium phosphate buffer solution were commercially purchased and used as received. Starting material $\{(\mu\text{-}SCH_2S)_2N(CH_2CO_2H)\}Fe_2(CO)_6$ was prepared according to the literature procedure.[1]

Elemental analysis (CHN) was done on the PerkinElmer 240C analyzer. Fourier transform infrared (FT-IR) spectroscopy was recorded on the Nicolet 670 FTIR spectrometer. Nuclear magnetic resonance (NMR) spectroscopy was recorded on the 600 MHz Bruker spectrometer. X-ray photoelectron spectroscopy (XPS) was recorded on ESCALAB 250Xi spectrometer with Al Kα radiation. Raman was performed on a Raman spectrometer with 532 nm laser excitation.

Crystal structure determination is performed as follows. Single crystals of diiron compound **1** (CCDC number 2415083) suitable for X-ray diffraction analysis were grown by slow evaporation of their CH_2Cl_2 solutions into hexane at −5°C. The crystals were mounted on a Bruker-CCD diffractometer. Data were collected at 193 (2) K using a graphite monochromator with Mo Kα radiation (λ = 0.71073 Å) in the ω–φ scanning mode. The structure was solved by direct methods using the SHELXS-97 program and refined by the full-matrix least-squares technique (SHELXS-97) on F^2.[2,3] Hydrogen atoms were located using the geometric method. The details of crystallographic data and structure refinement for **1** are listed in Table S1.

References:

[1] S.J. Wang, Y. Gao, X. Su, Y.Z. Wang, Y.P. Qu, P.H. Zhao, Aqueous pH influence on the electrocatalytic hydrogen evolution reaction with carbon nanotube-supported diiron dithiolato compound, Appl. Surf. Sci. 661 (2024) 160074.

[2] Sheldrick, G. M. A short history of SHELX. Acta Crystallogr. A 2008, 64, 112–122.

[3] Sheldrick, G. M. Crystal structure refinement with SHELXL. Acta Crystallogr. C Struct. Chem. 2015, 71, 3–8.

II. Synthesis of diiron compound 1 and functionalized carbon nanotubes CNT-COCl

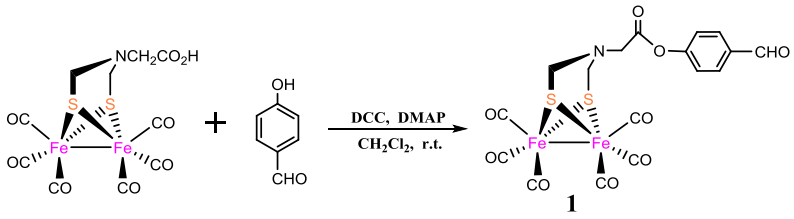

Scheme S1. Synthetic routes for diiron molecular compound **1**.

The synthetic procedure of compound **1** as shown in Scheme S1 is described as follows. A dry CH_2Cl_2 (20 mL) red solution containing the precursor compound (0.167 g, 0.40 mmol) and HOC_6H_4CHO-*p* (0.072 g, 0.60 mmol) were added with dehydrating agent DCC (0.083 g, 0.40 mmol) and catalyst DMAP (0.014 g, 0.12 mmol). This reaction mixture was stirred overnight at room temperature to produce brown-red solution. After the solvent was removed, the residue was separated by preparative thin-layer chromatography on silica gel eluting with CH_2Cl_2/petroleum ether (v/v = 10:1) and the main red band was collected to afford diiron compound **1**.

Compound **1**: Yield of 0.103 g (47%). Anal. Calcd for $C_{17}H_{11}Fe_2NO_9S_2$: C, 37.19; H, 2.02; N, 2.55%. Found: C, 37.13; H, 2.05; N, 2.49%. FT-IR (KBr, cm^{-1}): $\nu_{C\equiv O}$ 2074 (vs), 2032 (vs), 2019 (w), 1995 (s), 1974 (w); $\nu_{C(O)O}$ 1761 (s); ν_{CHO} 1694 (s). ^1H NMR (600 MHz, $CD3COCD_3$, TMS, ppm): δ_H 10.03 (s, 1H, CHO), 7.98 (s, 2H, C_6H_4), 7.34 (s, 2H, C_6H_4), 4.05 (s, 2H, NCH_2), 3.83 (s, 4H, 2 x SCH_2). $^{13}C\{^1H\}$ NMR (150 MHz, $CDCl_3$, TMS, ppm): δ_C 206.6 (Fe*C*O), 189.7 (*C*HO), 166.7 (*C*(O)O), 153.5, 133.3 (phenyl-*C*), 130.3, 121.0 (phenyl-*C*H), 57.9 (NCH_2), 51.7 (SCH_2).

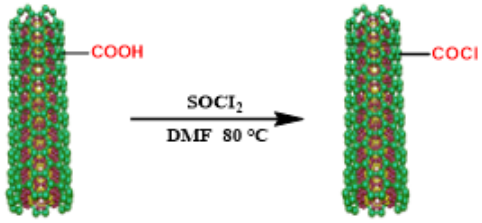

Scheme S2. Synthetic route for CNT-COCl

The synthetic procedure of CNT-COCl as shown in Scheme S2 is described as follows. Under the protection of N_2, 50 mg of carboxylated carbon nanotubes and 20 mL of $SOCl_2$ (0.275 mol) were added, 3-4 drops of DMF were added, and the black suspension was obtained by ultrasonic dispersion for 30 min, and the reflux reaction was carried out at 8°C for 24 h, and after filtration, it was dispersed by methanol ultrasonic, centrifuged and dried in vacuum to obtain 53.6 mg of black solid CNT-COCl.

III. Crystallographic data, spectroscopies, and electrochemistry of compound 1

Table S1. Details of crystallographic data and structure refinement for **1**

Compound	**1**
CCDC number	2415083
Empirical formula	$C_{17}H_{11}Fe_2NO_9S_2$
Formula weight	549.09
Temperature (K)	193(2)
Wavelength (Å)	0.71073
Crystal system	triclinic
Space group	P-1
a (Å)	8.9906(4)
b (Å)	9.5508(4)
c (Å)	13.0824(6)
α (°)	90.398(2)
β (°)	109.325(2)
γ (°)	91.029(2)
V (Å^3)	1059.79(8)
Z	2
D_{calc} (g cm^{-3})	1.721
μ (mm^{-1})	1.615
F(000)	552.0
Crystal size (mm)	0.32 × 0.28 × 0.24
θ_{min}, θ_{max} (°)	2.133, 30.496
Reflections collected/unique	40449/6429
R_{int}	0.0461
hkl Range	$-12 \le h \le 12$
	$-13 \le k \le 13$
	$-18 \le l \le 18$
Completeness to θ_{max} (%)	99.5
Data/restraints/parameters	6429/0/280
Goodness-of-fit (GOF) on F^2	1.064
R_1/wR_2 [$I > 2\sigma(I)$]	0.0264/0.0633
R_1/wR_2 (all data)	0.0335/0.0675
Largest difference peak/ hole (e A^{-3})	0.28/-0.54

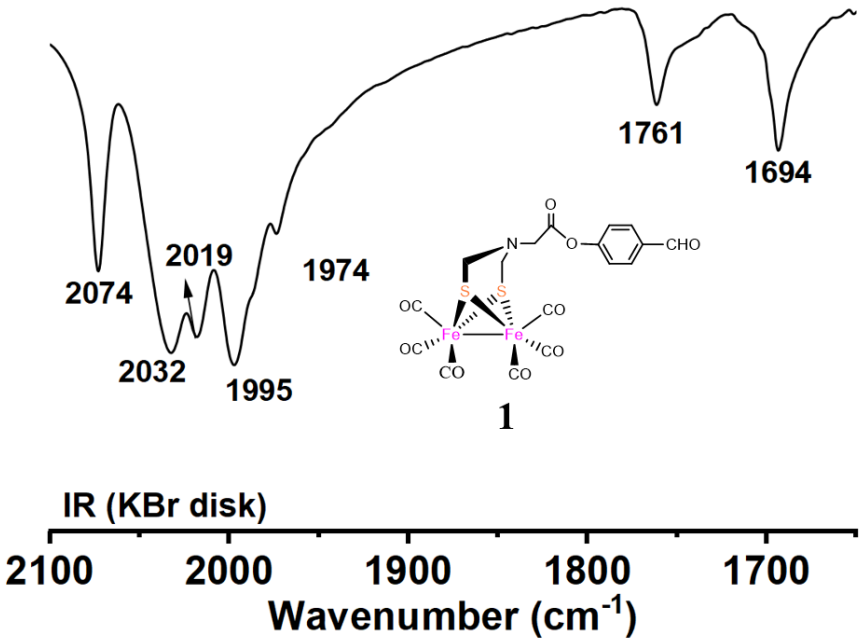

Figure S1. FT-IR spectrum (KBr disk) of compound **1**

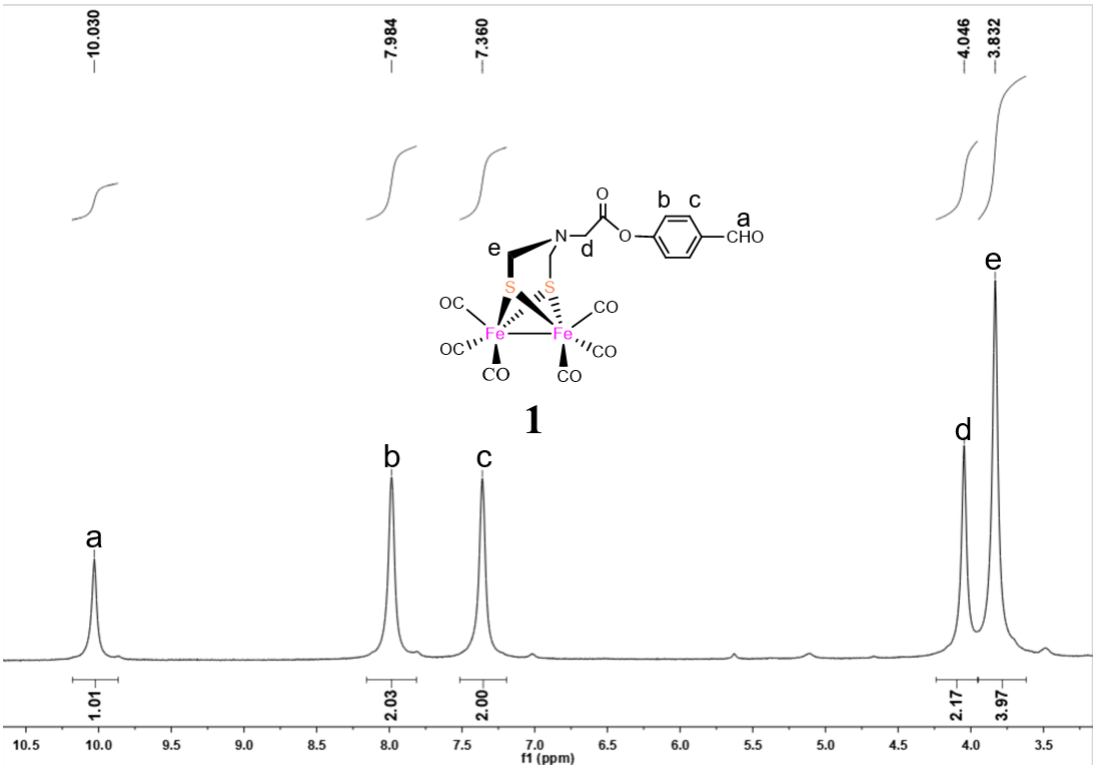

Figure S2. ^{1}H NMR (600 MHz, CD_3COCD_3, TMS) spectrum of compound **1**

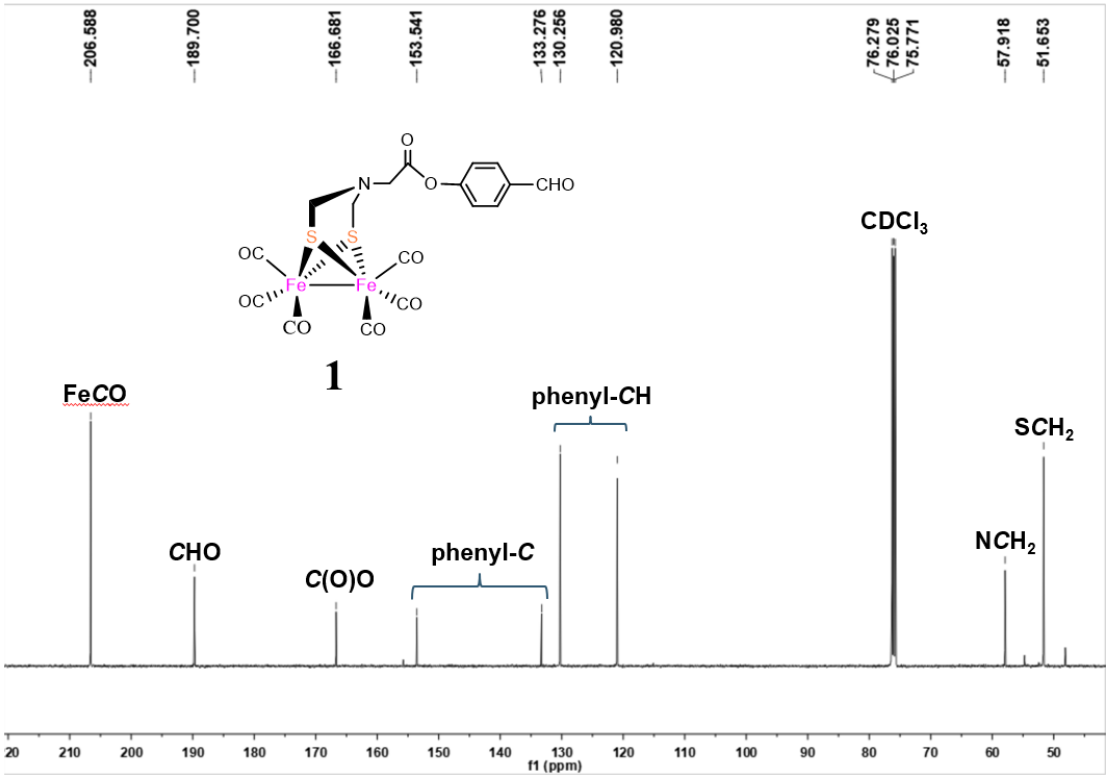

Figure S3. $^{13}C\{^{1}H\}$ NMR (150 MHz, $CDCl_3$, TMS) spectrum of compound **1**

IV. Additional spectroscopic data of CNT-supported hybrids CNT-X and CNT-X-ADT (X = N, C, O)

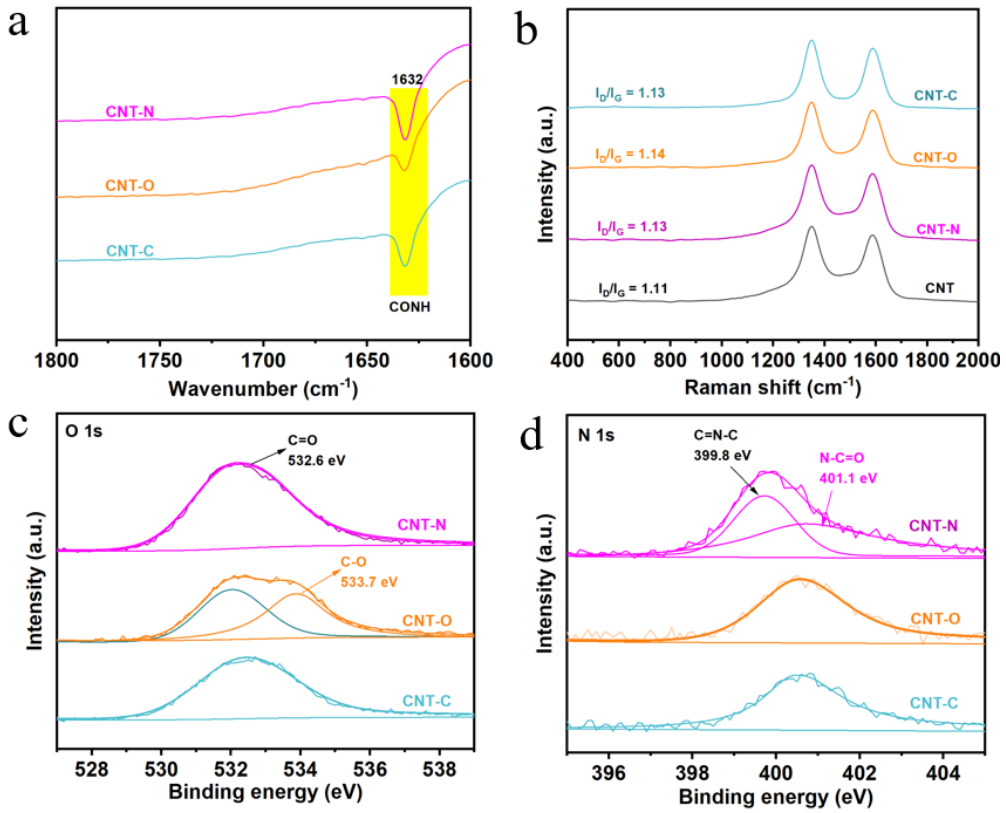

Figure S4. (a) FT-IR Spectra of **CNT-N** (purle), **CNT-C** (yellow), **CNT-O** (blue). (b) Raman spectra of **CNT-N** (purle)**, CNT-C** (yellow), **CNT-O** (blue) and pristine **CNTs** (black). (c-d) XPS Spectra for O 1s and N 1s analysis of **CNT-N** (purle)**, CNT-C** (yellow), **CNT-O** (blue).

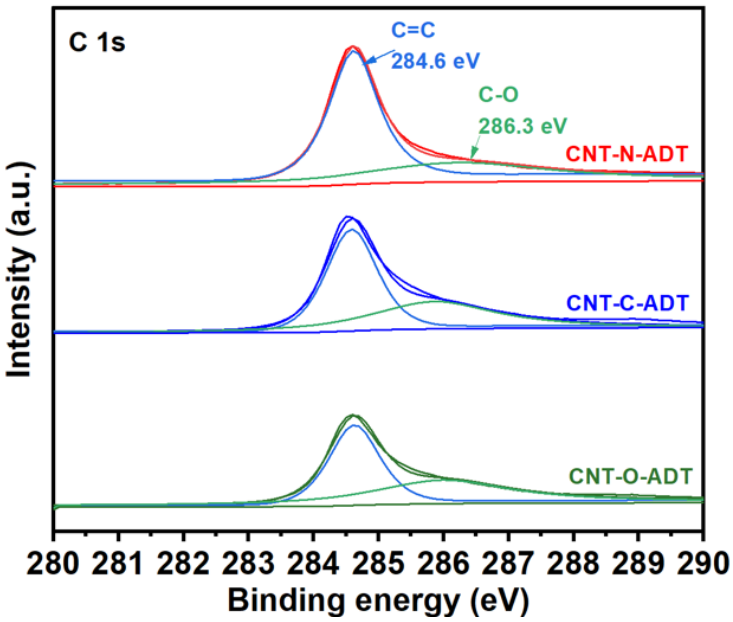

Figure S5. XPS Spectra for C 1s analysis of **CNT-N-ADT** (red)**, CNT-C-ADT** (blue), **CNT-O-ADT** (green).

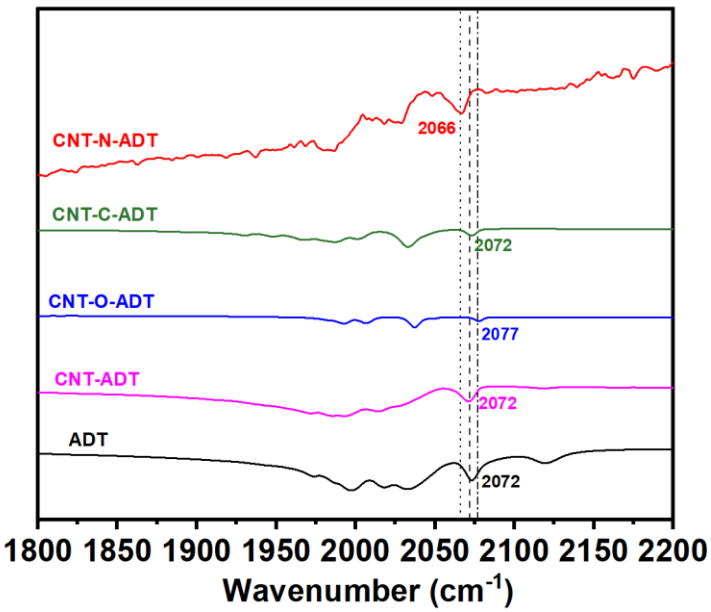

Figure S6. ATR-FR spectra of **CNT-X-ADT** (X= N, C, O) vs CNT-ADT vs. ADT

V. Additional electrochemical and electrolysis data of target hybrids CNT-X-ADT (X = N, C, O)

Table S2. Relevant electrocatalytic HER data of **CNT-X-ADT** and their reference samples

Hybrids	Overpotential (mV) at 10 mA cm^{-2}	Tafel slope ($mV\ dec^{-1}$)	R_{ct} (Ω)
CNT-N-ADT	880	102	111.2
CNT-C-ADT	970	129	120.3
CNT-O-ADT	1000	146	122.4
CNT-ADT	973	130	121.0
ADT	-	394	163.0
CNT-X	-	-	-
CNTs	-	-	-

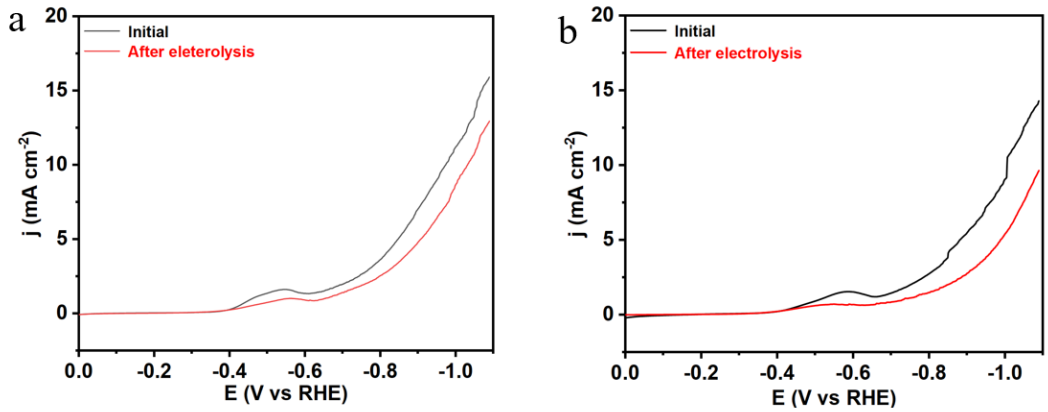

Figure S7. Lsv of a GC electrode loaded respectively with (a) **CNT-C-ADT** and (b) **CNT-O-ADT** before and after CA electrolysis.

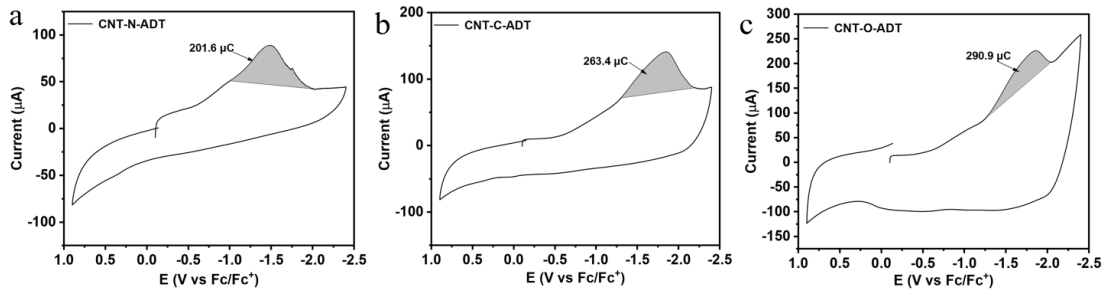

Figure S8. Cyclic voltammetry of hybrid catalysts (a) **CNT-N-ADT**, (b) **CNT-C-ADT**, (c) **CNT-O-ADT** (loading of 0.704 mg cm^{-2}) absorbed on GCE electrode in MeCN at a scan rate of 100 mV s^{-1} .

From the CV curve as shown in Figure S8, the charge of anodic peak integral is estimated to 2.016 x 10^{-4} C (**CNT-N-ADT**), 2.634 x 10^{-4} C (**CNT-C-ADT**), 2.909 x 10^{-4} C (**CNT-O-ADT**). Thus, we converted this charge to the moles of catalysts **CNT-X-ADT** on the GCE electrode (division by faraday constant), *i.e.*,

CNT-N-ADT: $n_{cat.}$ = Q/(F x 1) = 2.016 x 10^{-4} C/96485 C·mol^{-1} = 2.09 x 10^{-9} mol.

CNT-C-ADT: $n_{cat.}$ = Q/(F x 1) = 2.634 x 10^{-4} C/96485 C·mol^{-1} = 2.73 x 10^{-9} mol.

CNT-O-ADT: $n_{cat.}$ = Q/(F x 1) = 2.909 x 10^{-4} C/96485 C·mol^{-1} = 3.02 x 10^{-9} mol.

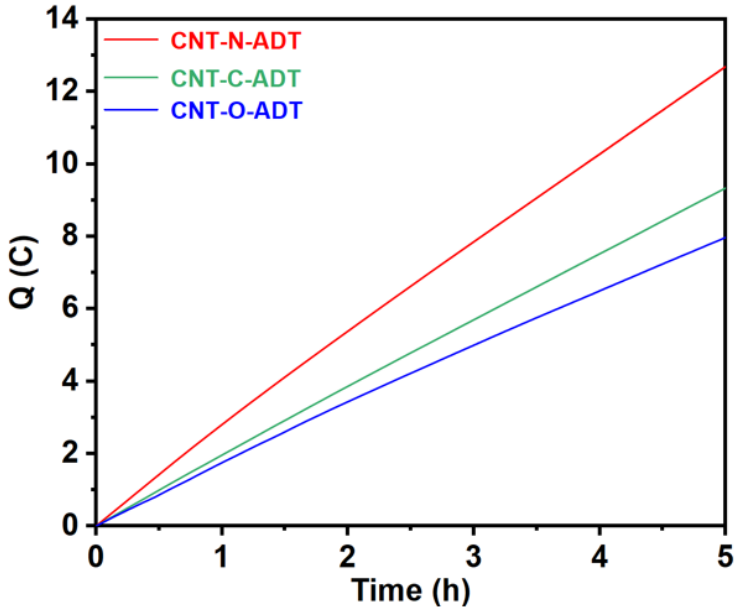

Figure S9. Chronoamperometry (CA) experiment of **CNT-N-ADT** (red) , **CNT-C-ADT** (green) , and **CNT-O-ADT** (red) electrodes with the same loading of 0.74 mg cm^{-2} consumed charge – time during 5 h electrolysis in 0.1 M phosphate buffer (pH = 7) aqueous solutions at the respective applied potentials of -0.88 V vs RHE.

Table S3. Relevant CA data of **CNT-X-ADT** in pH = 7 aqueous solution

Hybrid	HER stability			HER efficiency		
	Initial j (mA cm^{-2})	ultimately j (mA cm^{-2})	[a]Retention (%) of j	[b]Total charge (C) passed during 36 h CA	[b]Maximum TON_{H2}	Maximum TOF_{H2} (s^{-1})
CNT-N-ADT	11±0.3	9.3±0.2	85	12.68	3144	0.175
CNT-C-ADT	8±0.2	7.1±0.3	88	9.34	1771	0.098
CNT-O-ADT	7 ± 0.2	5.6 ± 0.2	80	7.96	1366	0.076

Note: (a) Retention (%) = (Initial j / uitimately j) x 100%. (b) Total charge (C) is obtained from the above Figure S9.